First-principles study of Ar adsorptions on the (111) surfaces of Pd, Pt, Cu, and Rh*

Niu Wen-Xia(牛纹霞)[a], Zhang Hong(张 红)[b]†, Gong Min(龚 敏)[b], and Cheng Xin-Lu(程新路)[a]

[a] Institution of Atomic and Molecular Physics, Sichuan University, Chengdu 610065, China
[b] College of Physical Science and Technology, Sichuan University, Chengdu 610065, China

(Received 30 June 2012; revised manuscript received 29 November 2012)

In the present paper we give a detailed report on the results of our first-principles investigations of Ar adsorptions at the four high symmetry sites on *M* (111) (*M* = Pd, Pt, Cu, and Rh) surfaces. Our studies indicate that the most stable adsorption sites of Ar on Pd (111) and Pt (111) surfaces are found to be the fcc-hollow sites. However, for Ar adsorptions on Cu (111) and Rh (111) surfaces, the most favorable site is the on-top site. The density of states (DOS) is analyzed for Ar adsorption on *M* (111) surfaces, and it is concluded that the adsorption behavior is dominated by the interaction between 3s, 3p orbits of Ar atoms and the d orbit of the base metal atoms.

Keywords: density-functional theory, binding energy, electronic structure

PACS: 68.43.–h, 68.43.Fg, 68.47.De, 65.40.gh **DOI:** 10.1088/1674-1056/22/6/066802

1. Introduction

Rare gas (RG) atoms have long been regarded as the classical adatoms for the study of physisorption mainly because of their notable inertness,[1] i.e., rare-gas atoms have closed shells, the simple electronic structures, and the weak interactions with surfaces.[2] As is well known, the adsorption for inert gas on a surface is generally weak, e.g., the binding energy of Xe/Pd (111)[3] is –453 meV. So it is typically assumed that the interaction between the adatoms and the metal surfaces is determined by an interplay between the van der Waals attraction and the Pauli repulsion,[2,4,5] and these systems have had a long tradition in serving as a model for obtaining a fundamental understanding of the process of adsorption.[6] High energy Ar ions have been used to clean solid surfaces and to measure local electrostatic fields.[7]

In the recent years, many researchers have obtained an improved understanding of the interaction between Xe atoms and metal surfaces. They have found that Xe adatoms preferentially bind to the low-coordinated on-top sites on metal surfaces, e.g., quantitative low-energy electron diffraction intensity analysis apparently have confirmed the on-top adsorption site for Xe adatoms on Cu (111), Pd (111), Ru (0001), and Pt (111) surfaces.[8–11] Furthermore, Seyller *et al.*[12] claimed that rows of Kr adatoms are located on top for Kr on Cu (110). In addition, from scanning tunneling microscopy there has been obtained the experimental evidence that Xe adatoms bind to the low coordination sites on Ni (110).[13] Recent low-energy electron diffraction (LEED) studies obtained the evidence for the on-top site preference for Ar/Ag (111).[14,15] In the present paper, we begin with studying the Ar adsorptions on *M* (111) (*M* = Pd, Pt, Cu, and Rh) surfaces. As is well known, there has been no experimental study of Ar adsorptions on these surfaces. Hence, it is necessary to understand first the atomic and the electronic structures of those systems.

2. Calculation method

The calculations described have been performed in the framework of the density functional theory (DFT)[16,17] as implemented in the CASTEP[18] package. Exchange and correlation were treated within the local-density approximation (LDA)[19] and generalized-gradient approximation (GGA) of Perdew, Burke, and Ernzerhof (PBE).[20] The electronic wave functions were expanded in a plane wave basis set, and the ionic cores were described by ultrasoft pseudopotentials.[21] In the present work, argon atoms are adsorbed at the four high symmetry sites: the top, bridge, fcc-, and hcp-hollow sites on *M* (111) surfaces. The positions of atoms in the two topmost *M* surface layers and the argon atoms are allowed to fully relax, but those on the remaining three metal layers are fixed. The *M* (111) surface is modeled by a unit cell, $p(2\times2)$, with five layers. The argon atom is adsorbed on one side of the slab only at a quarter monolayer coverage (0.25 ML). The vacuum region between slabs is 15 Å (1 Å = 0.1 nm) in size, and a cut-off energy of 300 eV is used. The Brillouin-zone integration is performed using a $(4\times4\times1)$ Monkhorst–Pack (MP) grid of *k*-points. The effects of the spin polarization for the systems are so small that they can be ignored in our calculations.

We address the stability of the Ar/metal structure with respect to adsorption of Ar by calculating the average binding energy per Ar adatom. The average binding energy, $E_b^{Ar/metal}$,

*Project supported by the National Natural Science Foundation of China (Grant No. 11074176), the National Natural Science Foundation of China (Grant No. 10976019), and the Research Fund for the Doctoral Program of Higher Education of China (Grant No. 20100181110080).

†Corresponding author. E-mail: hongzhang@scu.edu.cn

© 2013 Chinese Physical Society and IOP Publishing Ltd

is defined as[22]

$$E_{\rm b}^{\rm Ar/metal} = -\frac{1}{N_{\rm Ar}}[E^{\rm Ar/metal} - (E^{\rm metal} + N_{\rm Ar}E^{\rm Ar})], \quad (1)$$

where $N_{\rm Ar}$, $E^{\rm Ar/metal}$, $E^{\rm metal}$, and $E^{\rm Ar}$ are the number of Ar atoms in the surface unit cell, the total energies of the adsorbate-substrate system, the clean surface, and the isolated argon atom, respectively. A positive value of the binding energy indicates that the adsorption process is exothermic with respect to the free Ar atom, and a negative value shows that the process is endothermic.

The adsorption-induced dipole moment μ and the change of work function $\Delta\Phi$ are related by the Helmholtz equation, which in atomic units reads

$$\mu = \frac{A_{(1\times1)}}{12\pi\Theta}\Delta\Phi, \quad (2)$$

where $\Delta\Phi$ is the work-function change in unit eV, $A_{(1\times1)}$ is the surface area in an Å^2 per (1×1) surface unit cell, and Θ is the coverage in ML, i.e., 1/4 for the (2×2) structure. If $\Delta\Phi$ is given in eV, equation (2) yields an induced dipole moment in Debyes.

3. Bulk and clean surface

Before studying the effect of argon adsorptions on M (111) surface, we first calculate the property of the bulk metal system and analyze the metal surface structures in its most stable phases. The equilibrium lattice constants, bulk moduli, and cohesive energies are listed in Table 1, from which we find that the results of those physical quantities are in agreement with the experimental values. The values are also in-line with other reported results. In general, the PBE approximation yields the results in better agreement with experimental results. The surface relaxations for the clean surfaces are calculated with the LDA and PBE functional, and the calculation results are displayed in Table 2. The changes in the interlayer spacing for the two topmost atomic layers are obtained. The positive values indicate that atoms stretch outward; on the contrary, the negative values show that atoms contract inward. For Pd (111) surface, we find the changes in the interlayer spacing for the two topmost atomic layers with the LDA and PBE functionals are completely different. Using the LDA functional, the first and the second interlayer spacings are contracted by –0.12% and –0.16%, respectively, but using the PBE functional, no contraction is observed. A LEED analysis shows an expansion of the topmost interlayer spacing, e.g., $+1.3\pm1.3\%$.[31] It is indicated that it is able to obtain more accurate results through the use of the PBE functional. For the Pt (111) surface, we find that the first and the second interlayer spacings are contracted by –0.22% and –1.1% by using the LDA functional, respectively, and they are contracted by –0.3% and –2.1% by using the PBE functional, respectively. The work functions are also calculated and the results are listed in Table 2. However, on the whole, the results in Table 1, obtained by using the PBE functional are closer to the experiment values. Hence, only the results of PBE will be discussed below.

Table 1. Values of lattice constant a_0, bulk modulus B_0, and cohesive energy $E_{\rm coh}$.

Bulk		a_0/Å	B_0/Mbar	$E_{\rm coh}$/eV
Pd	LDA	3.86	2.46	–5.07
	PBE	3.95	1.58	–3.79
	Expt.[23]	3.89	1.81	–3.89
	Other PBE calculation[6]	3.95	1.63	–3.63
Pt	LDA	3.94	2.85	–7.29
	PBE	4.03	1.96	–5.79
	Expt.[23]	3.92	2.78	–5.84
	Other PBE calculation[6]	3.97	2.41	–5.59
Cu	LDA	3.55	1.27	–4.69
	PBE	3.68	1.23	–3.67
	Expt.[23]	3.61	1.37	–3.49
	Other PBE calculation[6]	3.63	1.42	–3.51
Rh	LDA	3.79	3.45	–8.59
	PBE	3.85	2.88	–7.11
	Expt.[24,25]	3.80	2.69	–5.75
	Other PBE calculation[26]	3.83	2.59	–6.10

Table 2. Relaxations of outermost layers for M (111), showing the values of the first (d_{12}) and the second (d_{23}) interlayer spacings, and the work function (Φ in eV).

Surface	d_{12}/Å		d_{23}/Å		Φ/eV		
	LDA	PBE	LDA	PBE	LDA	PBE	Expt.
Pd (111)	2.23	2.28	2.23	2.28	5.38	4.909	5.95[27]
Pt (111)	2.27	2.32	2.25	2.28	5.503	5.315	5.93[28]
Cu (111)	1.99	2.06	2.01	2.06	4.898	4.301	4.94[29]
Rh (111)	2.16	2.21	2.21	2.24	4.903	4.910	4.98[30]

4. On-surface adsorption

The adsorption models for Ar at the four high symmetry sites on M (111) surface are shown in Fig. 1 and the values of the binding energy $E_{\rm b}^{\rm Ar/metal}$ of the systems are plotted in Fig. 2 for Ar adsorption on the Pd (111) surface at the most favorable site with a binding energy of 59 meV, which is just 5 meV more favorable than on-top site. For Ar on the Pt (111) surface, the fcc-hollow site is energetically favorable with a binding energy of 31 meV, which is just 2 meV more stable than the on-top site. Our calculations demonstrate that the fcc-hollow site

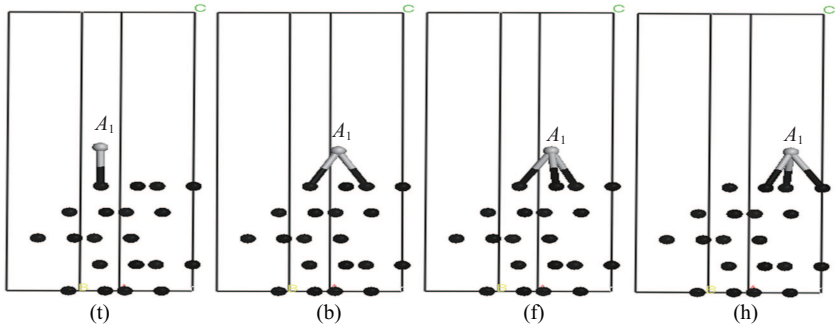


Fig. 1. Adsorption models at the top, bridge, fcc- and hcp-hollow sites on the *M* (111) surface respectively. The black ellipses represent the *M* atoms.

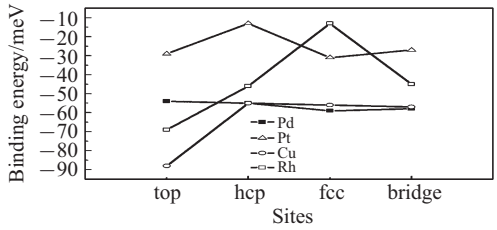


Fig. 2. Binding energies (in meV) of Ar adatoms at the four high symmetry sites on *M* (111) surface.

is more stable for Ar adsorption on Pd (111) and Pt (111) surfaces. For Cu (111) and Rh (111) surfaces, the adsorption situation of Ar is completely different. The binding energies of Ar adsorbed on-top sites of Pd (111) and Pt (111) surfaces are 32 meV and 56 meV more favorable than those at fcc-hollow sites for Cu (111) and Rh (111) surfaces, respectively. This indicates that the most stable sites of Ar adsorptions on Cu (111) and Rh (111) surfaces are the on-top sites; meanwhile, our binding energies for Ar on the Cu (111) surface are more accurate than other results.[32] In our previous work, we find that the fcc-hollow and hcp-hollow sites are the most favorable sites for the Ar/Al (111) and Ar/Ir (111) systems, respectively.[33]

In order to further analyze the most favorable adsorption site for the Ar adatom, we discuss the bond-lengths of Ar-metals, which are listed in Table 3. From Fig. 2, we can see the fcc-hollow site is more stable than the on-top site for Ar adsorption on the Pd (111) surface; meanwhile, a similar situation appears for the Ar/Pt (111) system. For the Ar/Cu (111) system, the bond-lengths for the on-top site and the fcc-hollow site are 3.135 Å and 3.603 Å, and for the Ar/Rh (111) system, the bond-lengths for the on-top site and the fcc-hollow site are 3.156 Å and 3.847 Å, respectively. This indicates the on-top site is more stable than the fcc-hollow site for Ar/Cu (111) and Ar/Rh (111). In order to check the effect of the adsorption stability of the surface substrate, we need to relax the topmost three metal layers (as compared with two metal layers) and fully relax the Ar atoms, and we find that the effect on the binding energy is almost negligible. For Ar adsorption on *M* (111), the four high symmetry sites are shown to be contracted to different extents, but the on-top site is shown to have a larger degree of contraction than the fcc-hollow site. For Ar atoms on Rh (111) surfaces, we find that the contraction of the topmost two interlayer spacings and the expansion of the second interlayer spacing are in different extents for the four high symmetry sites.

Table 3. Relevant geometric parameters (in Å) for Ar adsorption on *M* (111) surfaces.

Surface	Site	$d_{\mathrm{Ar-metal}}$/Å	d_{01}/Å	Δ_{12}/%	Δ_{23}/%
Pd (111)	top	3.359	3.359	–1.31	–1.75
	hcp	3.474	3.092	–0.44	–1.40
	fcc	3.435	3.074	–0.48	–0.87
	bridge	3.386	3.087	–0.53	–1.14
Pt (111)	top	3.517	3.517	–0.68	–2.19
	hcp	4.200	3.867	–0.43	–2.01
	fcc	3.884	3.556	–0.38	–2.02
	bridge	3.782	3.513	–0.60	–2.06
Cu (111)	top	3.135	3.135	–4.09	–3.52
	hcp	3.594	3.291	–3.67	–3.43
	fcc	3.603	3.293	–3.67	–3.15
	bridge	3.549	3.312	–3.85	–2.82
Rh (111)	top	3.156	3. 159	–0.67	0.72
	hcp	3.684	3.341	–0.63	0.58
	fcc	3.847	3.513	–0.62	0.76
	bridge	3. 587	3.337	–0.81	0.72

Note that $d_{\mathrm{Ar-metal}}$ is the bond-length between the Ar atom and the nearest metal atom. d_{01} is the vertical height of the Ar atom to the topmost metal layer. Δ_{12} is the change in distance between the first interlayer and the second metal interlayer, and Δ_{23} is the change in distance between the second layer and the third interlayer.

Turning now to the electronic properties, we analyze the work function change $\Delta\Phi$. Φ was proposed first by Einstein in his work on the photoelectric effect, which is defined as the minimum work required to remove a free electron from the interior of a solid to infinitely far away in vacuum.[34] Table 4 shows the induced work function change, $\Delta\Phi = \Phi^{\mathrm{Ar/metal}} - \Phi^{\mathrm{metal}}$. $\Delta\Phi$ can be related to the induced dipole moment μ using the Helmholtz equation. $\Delta\Phi$ and μ are related by a constant, hence, only the induced dipole moment will be discussed below. From Table 4, we can see that when Ar atoms are adsorbed at the fcc and the on-top sites on the Pd (111) surface, the absolute values of the induced dipole moment are very similar. For Ar on other systems, the absolute value (μ) of Ar atoms adsorbed at the most favorable site is larger than that at the second stable site, which is consistent with our results.

Table 4. Values of induced work function change and induced dipole moment μ for Ar/M (111) systems at the fcc-hollow and on-top sites. $\Delta\Phi$ and μ are given in eV and Debyes, respectively.

Ar/metal	Top		fcc	
	$\Delta\Phi$	μ	$\Delta\Phi$	μ
Pd (111)	–0.120	–0.086	–0.090	–0.064
Pt (111)	–0.090	–0.067	–0.146	–0.109
Cu (111)	–0.177	–0.110	–0.014	–0.009
Rh (111)	–0.368	–0.250	–0.103	–0.071

The charge population properties for Ar on M (111) at the fcc-hollow and the on-top sites are discussed and the results are detailed in Table 5. The Mulliken charge population analysis is implemented to analyze the charge transfer. As seen in Table 5, no matter whether Ar appears at the fcc-hollow site or the on-top site of the Ar/Pd system, the charge transfer is the same. Therefore, we know that the adsorption situations of Ar on Pd (111) at the fcc-hollow and the on-top sites are very close. For Ar/Pt system, when Ar appears at the favored site, the charge transfer is about 0.02 e, a similar value of 0.01 e is seen for Ar adsorbed at the on-top site. For Ar/Cu and Ar/Rh systems, the charge transfer, when Ar adsorption occurs at the fcc-hollow site, is a little smaller than that at the on-top site. Furthermore, it indicates that the on-top site is the most favorable site for Ar adsorptions on Cu (111) and Rh (111) surfaces, and the fcc-hollow site for Pt (111) surface.

Table 5. Mulliken charge quantities (in units of e) of Ar atoms adsorbed at the fcc-hollow and on-top sites.

Surface	Site	Ar-3s	Ar-3p	Charge
Pd (111)	top	2.00	5.97	0.03
	fcc	2.00	5.97	0.03
Pt (111)	top	2.00	5.99	0.01
	fcc	2.00	5.98	0.02
Cu (111)	top	2.00	5.97	0.03
	fcc	2.00	5.98	0.02
Rh (111)	top	2.00	5.96	0.04
	fcc	2.00	5.99	0.01

The charge transfer situations of Ar on M (111) surfaces at the fcc-hollow and the on-top sites are also reflected in the electron density difference (Fig. 3). The black areas represent charge loss, and the white zones denote the charge accumulation. The tangent plane is the (001) plane occupied by the Ar atoms and the nearest neighboring metal atoms. From Fig. 3 we find the formation of an Ar–M bond and this is a polarization of the surface M atoms. For the Ar/Pd system, we find the increase of charge density of Ar atoms at the on-top site is bigger than that at the fcc-hollow site. For the Ar/Pt system, the difference is that the increment of charge density of Ar at the fcc-hollow site is bigger than that at the on-top site. It indicates that the fcc-hollow site is the most favorable site. From the Ar atoms on Cu (111) and Rh (111) surfaces, we find the increment of charge density of Ar at the on-top site is bigger than that at the fcc-hollow site. It indicates that the on-top sites are the more favorable sites of Ar atoms on Cu (111) and Rh (111) surfaces.

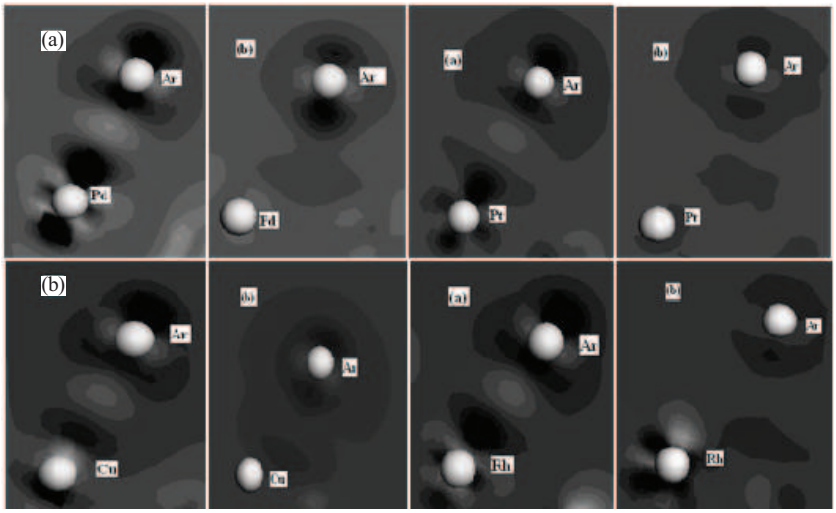


Fig. 3. Electron density difference plots of Ar adsorption on the M (111) surface at the on-top and fcc-hollow sites. The panel (a) shows Ar at the on-top site and panel (b) indicates Ar at the fcc-hollow site.

The densities of states (DOSs) for Ar/*M* (111) systems have been discussed as shown in Fig. 4. For Ar on the Pd (111) surface, we can see that the DOS mainly consists of a Pd (111) 4d orbit. A prominent new peak appears at about 19.3 eV below the Fermi level, the peak at about 5.8 eV below the Fermi level is enhanced, an effective (bonding) hybridization between Pd-4s and 4d states at about 5.0 eV below the Fermi level and an effective hybridization between Pd-4d and 4p states at about 1.0 eV above the Fermi level. However, we find that the total densities of states (TDOSs) of Ar adsorbed at the two sites are very similar. For Ar on the Pt (111) surface, orbital hybridization takes place in Ar and Pt atoms. However, There is a minor difference between the two sites, the TDOS for Ar adsorbed at the fcc-hollow site is higher than that at the on-top site at about 4.0 eV below the Fermi level, which indicates that Ar adsorbed at the fcc-hollow site is more stable. For Ar on the Cu (111) surface, the same situation of Ar on the Pd (111) surface occurs in Ar on the Cu (111) surface. For Ar on the Rh (111) surface, there is a notable difference between those two sites, i.e., the TDOS for Ar adsorbed at the on-top site is higher than that at the fcc-hollow site at about 5.5 eV below the Fermi level, which indicates that Ar adsorbed at the on-top site is more stable.

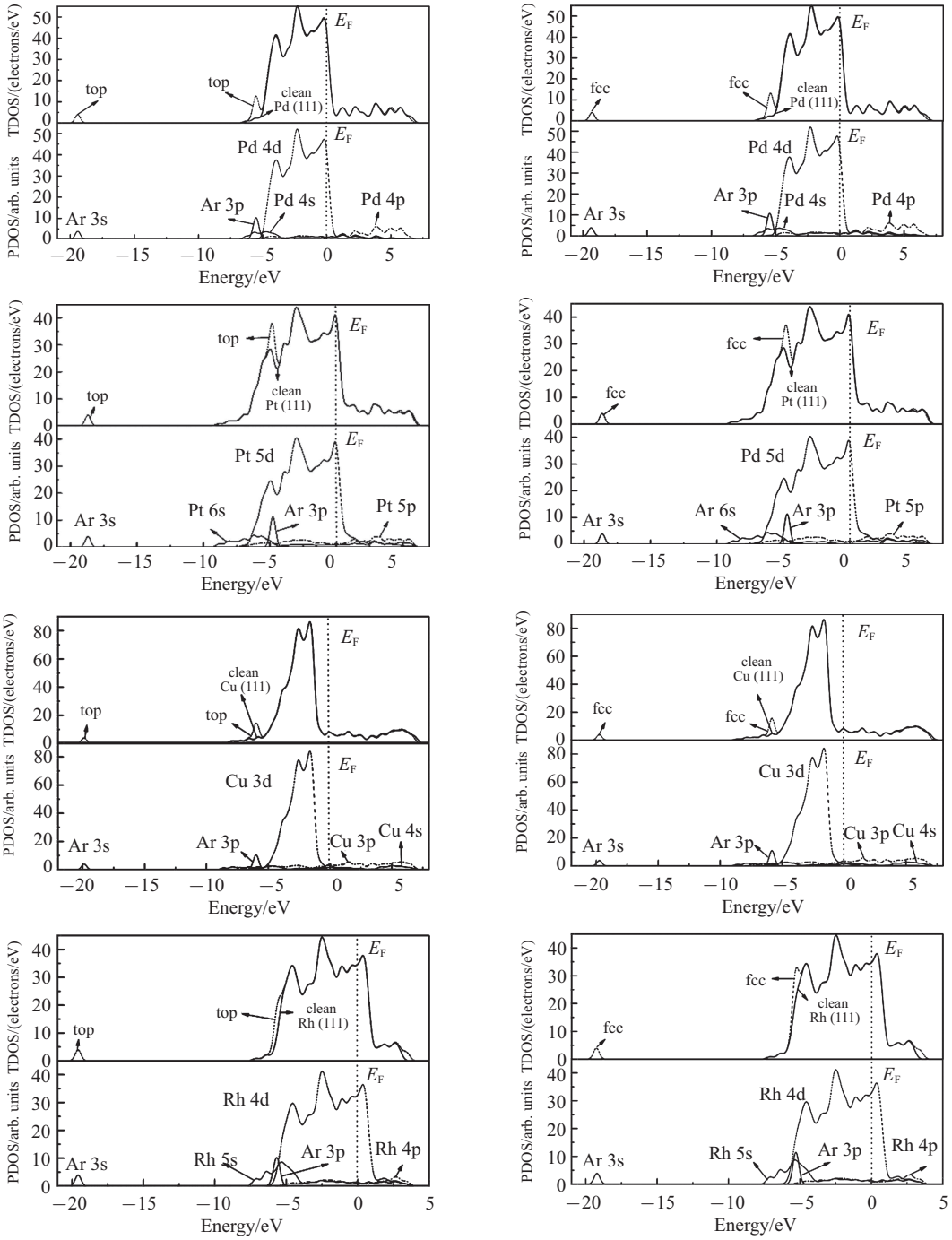


Fig. 4. Densities of states of Ar on *M* (111) at the top and fcc sites. The energy reference is the Fermi energy (0 eV). Here, TDOS and PDOS stand for total density of states and projected density states, respectively.

5. Conclusions

Using DFT, the adsorptions of Ar on *M* (111) surfaces are studied in this work. It can be seen that Ar atoms adsorbed at the fcc-hollow and on-top sites on those metal surfaces are more stable. The difference is that Ar atoms adsorbed at the fcc-hollow site on Pd (111) and Pt (111) surfaces are more stable than that at the on-top site; meanwhile, the on-top site is more stable than the fcc-hollow site when Ar adsorptions take place on two other surfaces. Furthermore, from the DOS we can see that the results are due mainly to the interaction between 3s, the 3p orbits of Ar atom and the d orbit of the base metal atoms; meanwhile, from the projected density of states (PDOSs) we find that the fcc-hollow site is more stable for Ar adsorptions on Pd (111) and Pt (111) surfaces, and the on-top site is more stable for Ar adsorptions on Cu (111) and Rh (111) surfaces.

References

[1] Li Sh, Yuriko O and Tetsuya T 2010 *J. Phys. Chem. C* **114** 3544
[2] Bruch L W, Cole M W and Zaremba E 1997 *Physical Adsorption: Forces and Phenomena* (Oxford: Oxford Science Press)
[3] Juarez L F, Da Silva, Catherine S and Matthias S 2003 *Phys. Rev. Lett.* **90** 066104
[4] Desjonquères M C and Spanjaard D 1995 *Concepts in Surface Science* (New York: Springer)
[5] Vidali G, Ihm G, Kim H Y and Cole M W 1991 *Surf. Sci. Rep.* **12** 135
[6] Juarez L F, Da Silva, Catherine S and Matthias S 2005 *Phys. Rev. B* **72** 075424
[7] Juarez L F, Da Silva and Catherine S 2008 *Phys. Rev. B* **77** 045401
[8] Seyller Th, Caragiu M, Diehl R D, Kaukasoina P and Lindroos M 1998 *Chem. Phys. Lett.* **291** 567
[9] Caragiu M, Seyller Th and Diehl R D 2002 *Phys. Rev. B* **66** 195411
[10] Narloch B and Menzel D 1997 *Chem. Phys. Lett.* **290** 163
[11] Seyller Th, Caragiu M, Diehl R D, Kaukasoina P and Lindroos M 1999 *Phys. Rev. B* **60** 11084
[12] Seyller Th, Caragiu M and Diehl R D 2000 *Surf. Sci.* **454** 55
[13] Weiss P S and Eigler D M 1992 *Phys. Rev. Lett.* **69** 2240
[14] Diehl R D, Seyller Th, Caragiu M, Leatherman G S, Ferralis N, Pussi K, Kaukasoina P and Lindroos M 2004 *J. Phys.: Condens. Matter* **16** S2839
[15] Caragiu M, Letherman G S, Seyller Th and Diehl R D 2001 *Surf. Sci.* **475** 89
[16] Hohenberg P and Kohn W 1964 *Phys. Rev.* **139** 864
[17] Kohn W and Sham L J 1965 *Phys. Rev.* **140** 1133
[18] Clark S J, Segall M D, Pickard C J, Hasnip P J, Probert M J, Refson K and Payne M C 2005 *Zeitschrift Fur Kristallographie* **220** 567
[19] Perdew J P and Wang Y 1992 *Phys. Rev. B* **45** 13244
[20] Perdew J P, Burke K and Ernzerhof M 1996 *Phys. Rev. Lett.* **77** 3865
[21] Wang M M, Ning H, Tao X M and Tan M Q 2011 *Acta Phys. Sin.* **60** 047301 (in Chinese)
[22] Scheffler M and Stampfl C 2000 "Theory of Adsorption on Metal Substrates", in: Horn K and Scheffler M ed. *Handbook of Surface Science*, Vol. **2**. *Electronic Structure* (Amsterdam: Elsevier) pp. 286–357
[23] Kittel C 1996 *Introduction to Solid State Physics*, 7th edn. (New York: Wiley)
[24] Villars P and Calvert L D 1985 *Pearson's Handbook of Crystallographic Data for Intermetallic Phases* (ASM: Metals Park)
[25] Kittel C 1986 *Introduction to Solid State Physics,* 6th edn. (New York: Wiley)
[26] Ganduglia-Pirovano M V and Scheffler M 1999 *Phys. Rev. B* **59** 15533
[27] Wandelt K and Hulse J E 1984 *J. Chem. Phys.* **80** 1340
[28] Zeppenfeld P 2001 *Physics of Covered Solid Surfaces Group III*, Vol. **42** (Berlin: Springer-Verlag) p. 67
[29] Hölzl J, Schulte F K and Wagner H 1979 "Work Function of Metals," in *Solid State Physics, Springer Tracts Modern Physics* Vol. **85** (Berlin: Springer)
[30] Lide D R 1995 *CRC Handbook of Chemistry and Physics*, 76th edn. (Boca Raton: CRC Press) pp. 12–123
[31] Ohtani H, Van Hove M A and Somarjai G A 1987 *Surf. Sci.* **187** 372
[32] Silvestrelli P L, Ambrosetti A, Grubisic S and Ancilotto F 2012 *Phys. Rev. B* **85** 165405
[33] Niu W X and Zhang H 2012 *Chin. Phys. B* **21** 026802
[34] Li W and Li D Y 2005 *J. Chem. Phys.* **122** 064708